Available online at www.sciencedirect.com
ScienceDirect
Journal of the European Ceramic Society 31 (2011) 921–930
www.elsevier.com/locate/jeurceramsoc

Wear properties of α- and α/β-SiAlON ceramics obtained by gas pressure sintering and spark plasma sintering

S. Kurama [a,*], I. Schulz [b], M. Herrmann [c]

[a] *Anadolu University, Department of Materials Science and Engineering, 26555 Eskisehir, Turkey*
[b] *Technical University Dresden, Institute of Material Science, Dresden, Germany*
[c] *Fraunhofer Institute for Ceramic Technologies and Systems, D-01277 Dresden, Germany*

Received 20 January 2010; received in revised form 31 October 2010; accepted 21 November 2010
Available online 18 December 2010

Abstract

In this study, α- and α/β-SiAlON materials, doped with Y_2O_3 and Nd_2O_3, were sintered using two different sintering processes: spark plasma sintering (SPS) and gas pressure sintering (GPS). The wear and mechanical properties of the samples were compared related to the composition, additives and sintering processes. The results show that the hardness was not affected by the processing type whereas the toughness values were lower for spark plasma sintered materials than gas pressure sintered materials. This can be explained by the changed microstructure of the two different types of material. Additionally, α/β-SiAlON materials, sintered using gas pressure sintering, showed a lower wear than the spark plasma sintered materials. The results of the wear test were compared with β-Si_3N_4 materials and it was observed that α/β-SiAlON, sintered by GPS, has better wear properties than the tested β-Si_3N_4 materials.

Keywords: Grain boundary phase; Wear resistance; SiAlON; Wear parts; Cutting tools

1. Introduction

Nowadays, SiAlON ceramics are widely used in high temperature industrial, automotive and aerospace applications, such as in cutting tools, wire drawing, dies and blast nozzles.[1–3] There are two well-known kinds of SiAlON. α-SiAlON and β-SiAlON, which are solid solutions based on α- and β-Si_3N_4, respectively. These ceramics are generally produced using oxide and nitride additives to enhance their densification. However, the remaining amorphous phase softens at high temperatures and results in a deleterious effect on the high temperature strength, and oxidation properties.[4–7] With the aim of improving SiAlON ceramics properties, efforts have focused on controlling the grain boundary chemistry, either by reducing the impurity contents of the glass,[8] by adding more glass-forming refractory oxides[9–13] as sintering additives, or by crystallizing the intergranular phases through post heat treatment.[14] The minimization of the intergranular amorphous phase in SiAlON materials allows for an improvement in the wear and friction properties of SiAlON ceramics. Recent studies show that the wear properties of yttrium based SiAlON ceramics, containing high amounts of β-SiAlON, are better than for α-SiAlON, whereas this condition is reversed under mild wear conditions due to the lower amount of the grain boundary phase in the α-SiAlON microstructure.[15–17] However, a relatively recent development in the field of α-SiAlON materials is the enhancement of microstructures with elongated grains by improving the fracture toughness.[18] The improvement of the fracture toughness of α-SiAlON ceramics can be achieved with microstructural control during sintering. The development of such microstructures is most commonly achieved through the seeding of the starting powders[19] using starting compositions which result in extended transient liquid formation[20] and/or rapid sintering techniques, such as spark plasma sintering, SPS.[21] SPS is a comparatively new sintering process. This technique has significant advantages over conventional sintering techniques. In the SPS method, raw powders in a carbon die are pressed uniaxially, with a direct current (dc) pulse voltage being applied. The pulsed direct current is allowed to pass through the electrically conducting pressure die as well as the material (if it is conducting). Therefore, rapid heating is available and the sintering time can be shortened. The SPS technique has been widely

* Corresponding author. Tel.: +90 222 321 3550x6372; fax: +90 222 323 9501.
E-mail addresses: semra.kurama@gmail.com, skurama@anadolu.edu.tr (S. Kurama).

0955-2219/$ – see front matter © 2010 Elsevier Ltd. All rights reserved.
doi:10.1016/j.jeurceramsoc.2010.11.010

used to produce a wide range of ceramics, including oxides[22–24] and nitrides.[23–27]

In a recent account of the wear properties of yttrium based SiAlON ceramics, it was shown that wear behaviour depends significantly on the microstructure and chemical stability of the materials.[16] In this work, two different α- and α/β-SiAlON compositions, doped with Y_2O_3 or Nd_2O_3, were sintered using the gas pressure sintering and the spark plasma sintering processes. The effect of the sintering type and the additive on wear behaviour is discussed related to the starting composition. The results are compared with two β-Si_3N_4 materials.

2. Experimental studies

2.1. Material preparation and characterisation

Two starting compositions of α- and α/β-SiAlON, doped with Y_2O_3 or Nd_2O_3 (99.99% HC Starck) additives, were prepared using Si_3N_4 (UBE-10, containing 1.6% oxygen), AlN (Tokuyama, containing 1% oxygen), Al_2O_3 (99.99%, Sumitomo AES IIC), Y_2O_3 and Nd_2O_3 powders. When calculating the overall composition, the oxides (according to the manufacturers' specifications) on the surface of Si_3N_4 and AlN powders were taken into account.

The starting powders were weighed and milled in water-free isopropanol for 90 min using an agate milling media. The mixed powders were dried and isostatically pressed into bars (of dimensions 60 mm × 20 mm × 20 mm) under a pressure of 200 MPa for gas pressure sintering (GPS). The sintering of the materials was carried out by GPS and spark plasma sintering (FAST HPD25; FCT Germany) under nitrogen atmosphere at 1825 °C for 90 min (3 MPa) and 1750 °C for 5 min (20 MPa), respectively. Y_2O_3 and Nd_2O_3 were chosen as the sintering additives owing to their different ionic radiuses and stabilization behaviour in the α-SiAlON structure.

To show the effect of starting composition on wear behaviour of SiAlON ceramics two different types of starting composition were selected. One of the compositions was selected in the α/β-SiAlON region ($m = 0.5$ and $n = 1.0$). The other composition was selected within the single α-SiAlON region ($m = 1.25$ and $n = 1.0$). The designation of the materials is given in Table 1.

In order to develop an elongated grain structure and to investigate the grain boundary phase effect on mechanical and wear properties, an additional liquid phase during sintering was formed by the addition of Y_2O_3 and Nd_2O_3 (2 wt.% excess). These additives remain as the grain boundary phase. In addition, two different Si_3N_4 materials, hot pressed at 1700 and 1850 °C with 11 wt.% of amorphous phase (6 wt.% Y_2O_3 and 5 wt.% Al_2O_3), were selected as reference materials.

The surface of the sintered materials was removed (at least 4 mm) and then the phase composition was analysed using the X-ray diffraction technique (XRD 7 Seifert, FPM; Cu Kα). A quantitative XRD analysis was made with the programme REFINE++ (Seifert FPM).[28] A microstructural characterisation and a worn surface analysis were performed with a field emission scanning electron microscope (FESEM, Leo 982, Stuttgart, Germany).

The mechanical properties were assessed through measurements of the hardness and fracture toughness. Vickers hardness tests were carried out under 98 N. The fracture toughness (K_{IC}) was determined using the indentation-fracture (IF) method using the Anstis equation[29] under the same load. In both cases the results are presented as the average of five separate measurements.

2.2. Wear test

After sintering, the samples were ground and polished using 6 μm diamond grains to a surface roughness of $R_a = 0.04$ μm. Following this procedure, friction and wear tests were conducted under dry conditions on a computer controlled tribometer SRV III (Optimol Instruments GMBH, Germany) in ball-on-disk configurations under a reciprocating sliding motion. The materials were tested against a steel ball bearing (100Cr6, Ø10 mm) at room temperature. Experiments were conducted inside a climatic chamber keeping a constant relative humidity of 50% and a temperature of 22 °C. The sliding speed was 0.1 m/s and the load ranged from 10 to 30 N. Each test pair had a 60 min running time under selected speed and loads. These tests were each repeated twice. Before testing, the materials were ultrasonically cleaned in an acetone bath for 5 min.

The wear scare length at the plate was measured using a light microscope. The cross section of the wear scare at the plate was measured by using a profilometer and then the volume and wear rate, w, were calculated. The friction force, F_f, was transmitted by a transducer to a recorder continuously during the testing, from which the friction coefficient, μ, was obtained.

3. Results

3.1. Sintering behaviour of samples

According to Table 2, SPS sintered materials (except for N2) have the same density as the GPS materials. Even though the materials were sintered at a lower temperature (1750 °C) and for a shorter time (5 min), by the SPS sintering, they had a higher amount of the α-SiAlON phase than that of those gas pressure sintered. The results of XRD analyze are given in Table 2 revealed that both of the ($m = 1.25$ and $n = 1.0$) compositions, doped with Nd_2O_3 and Y_2O_3, resulted in single phase α-SiAlON, whilst for the ($m = 0.5$, $n = 1.0$) compositions β-SiAlON was also observed as it was expected. The additional additive using, to increase density of samples, was not significantly effect the phase composition of these samples (N1, Y1, N1-E2 and Y1-E2). These additional additives were stayed in the structure as an amorphous phase after the consummation of the densification of samples. However, the α/β-SiAlON composition ($m = 0.5$, $n = 1.0$) has different amount of β-SiAlON phase related with the type of sintering method. XRD phase analyze results of the samples, sintered by GPS, are more reliable than that of SPS. Due to fast cooling rate of SPS the α ↔ β-SiAlON transformation was prevented and the compo-

Table 1
Material designations and compositions.

Sample	*m*	*n*	Additive		Excess Nd_2O_3 (2 wt.%)	Excess Y_2O_3 (2 wt.%)
			Nd_2O_3	Y_2O_3		
N1	1.25	1.0	•			
N1-E2	1.25	1.0	•		•	
N2	0.5	1.0	•			
N2-E2	0.5	1.0	•		•	
Y1	1.25	1.0		•		
Y1-E2	1.25	1.0		•		•
Y2	0.5	1.0		•		
Y2-E2	0.5	1.0		•		•
485-Si_3N_4[a]						
480-Si_3N_4[b]						

[a] Sintered at 1850 °C.
[b] Sintered at 1700 °C.

sition of sintered SiAlON shifted from starting composition. On the other side the samples, sintered by GPS, stayed the starting composition. Therefore its phase ratio is ∼55 wt.% α-SiAlON–45 wt.% β-SiAlON for sample N2. The addition of excess amount of additive also resulted with significant change in phase composition of SiAlON (N2-E2), sintered by GPS.

3.2. The effect of the starting composition and amount of additive on friction and wear behaviour

Figs. 1 and 2 show the variations of the friction coefficients and wear rates with load under dry conditions for materials sintered using both sintering processes, respectively. It can be seen that the friction coefficient and wear rate of the plate decreases with increasing load for both types of sintered material. The results of SPS sintered samples (N1 and N2), doped with Nd_2O_3, showed that starting composition has an significant effect on the wear behaviour (the higher amount of α-SiAlON phase the lower friction coefficient) of SiAlON under low load (10 N) whereas this difference decreased under higher loads (20 and 30 N). On the other side the friction coefficient of GPS's sample (N1) is higher (change between 1.4 and 0.9) than that of SPS (change between 1.1 and 0.95). This difference is also observed in Y_2O_3 doped samples (Y1-E2 and Y2-E2). The presence of β-SiAlON phase positively affected the friction resistance of Y2-E2 samples compare to sample Y1-E1 for both of sintering method. This result obtained thanks to morphology and amount of β-SiAlON phase.

In the spark plasma sintered α-SiAlON composition (N1 and N1-E2), increasing the amount of additives results in an increasing wear rate. Thus, the amorphous grain boundary phase deteriorated the wear properties of the materials. However, the excess amount of additive effect was not so pronounced in the gas pressure sintered materials (N1 and N1-E2).

The wear test of SiAlON materials were investigated against a steel ball bearing (100Cr6, Ø10 mm) at room temperature. During the wearing test steel ball also was worn by SiAlON materials, related with the starting composition and sintering method. The photos of wear surface of selected samples are given in Fig. 3. The wearing areas of steel balls were calculated and results are in agreed with the friction coefficient of SiAlON samples. The steel ball, used against to SPS-sintered samples, was worn more than that of GPS-sintered.

Table 2
The density and XRD results of materials.

Sample	Theoretical *x*-values	SPS			GPS		
		Phases (wt.%)	Calculated *x*-value	Density (g/cm^3)	Phases (wt.%)	Calculated *x*-value	Density (g/cm^3)
N1	0.42	α-SiAlON	0.48 ± 0.01	3.41	α-SiAlON	0.36 ± 0.01	3.40
N1-E2	0.42	α-SiAlON	0.52 ± 0.01	3.44	α-SiAlON	0.38 ± 0.01	3.44
N2	0.17	75.5 α-SiAlON ± 0.3 24.5 β-SiAlON ± 0.3	0.25 ± 0.01	3.26	55.4 α-SiAlON ± 0.3 44.6 β-SiAlON ± 0.3	0.28 ± 0.01	2.37
N2-E2	0.17	76.9 α-SiAlON ± 0.3 23.0 β-SiAlON ± 0.3	0.30 ± 0.01	3.31	74.4 α-SiAlON ± 0.4 25.6 β-SiAlON ± 0.4	0.26 ± 0.01	3.29
Y1-E2	0.42	α-SiAlON	0.40 ± 0.01	3.31	α-SiAlON	0.41 ± 0.01	3.31
Y2-E2	0.17	86.5 α-SiAlON ± 0.2 13.5 β-SiAlON ± 0.2	0.23 ± 0.01	3.24	81.1 α-SiAlON ± 0.3 18.9 β-SiAlON ± 0.3	0.25 ± 0.01	3.24

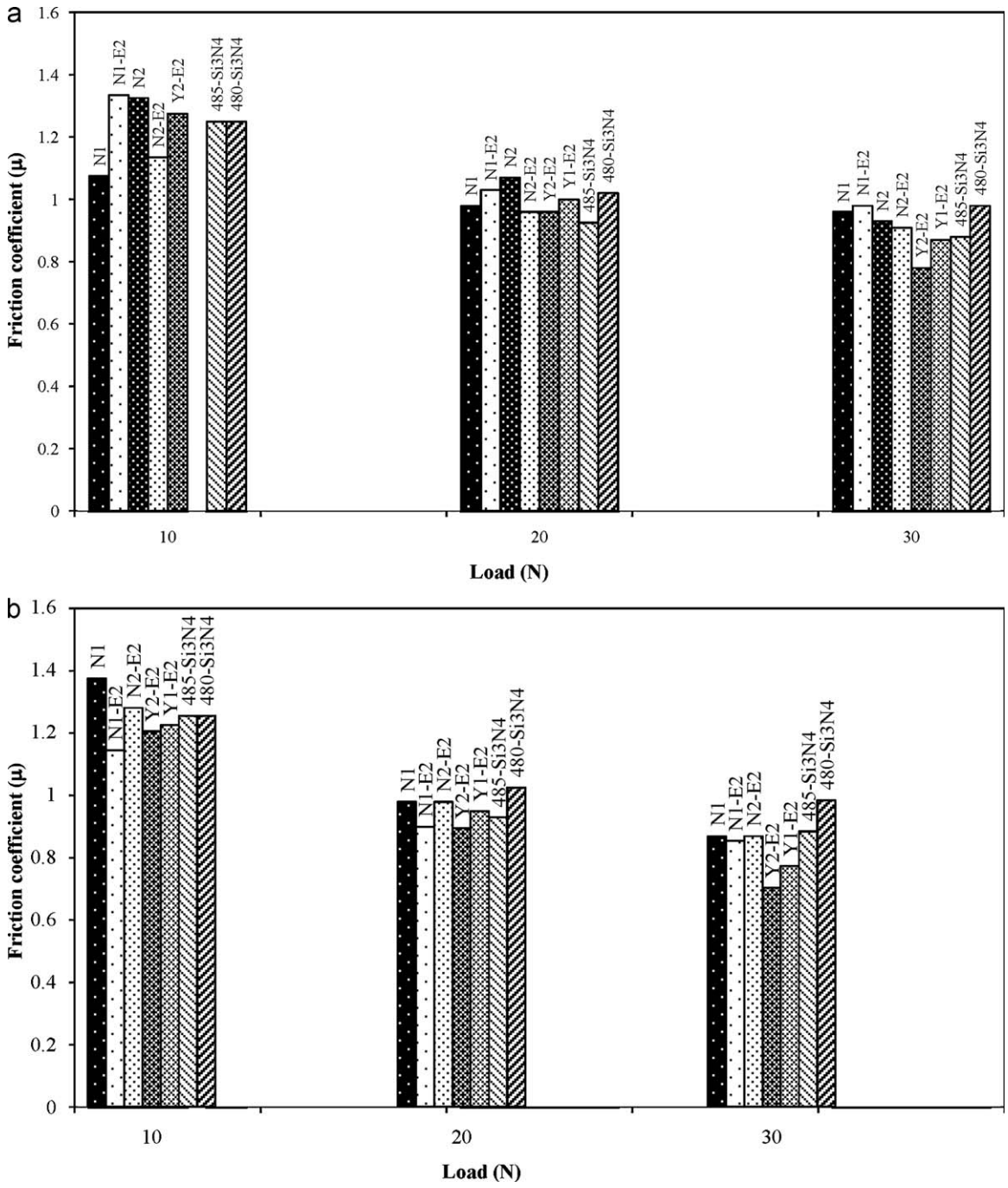

Fig. 1. Variation of friction coefficient with load in (a) spark plasma sintered materials and (b) gas pressure sintered materials.

3.3. The effect of the microstructure and mechanical properties on friction and wear behaviour

In the corresponding SPS and gas pressure sintered materials, the different degree of grain boundary phase was observed, with different wear behaviour. The sample N1, sintered with SPS, has more wear resistance (Figs. 1 and 2) than that of GPS sintered even though the former has more grain boundary phase (Fig. 4a and b). This result can be explained with the microstructure differences of samples. The comparable gas pressure sintered materials generally have a coarser microstructure and higher fracture toughness in comparison to materials sintered using SPS.

For all materials, the stainless steel adhered to the ceramic surface at low load more often than at high load in dry conditions. The material Y2-E2 showed the best wear properties for both sintering processes, whilst the material N1 performed the worst. The wear surfaces of the Y2-E2 and N1 materials were investigated using FESEM microstructural analysis. By increasing the load, no significant differences could be observed in the worn material surfaces. The results for 30 N load applications are given in Fig. 5.

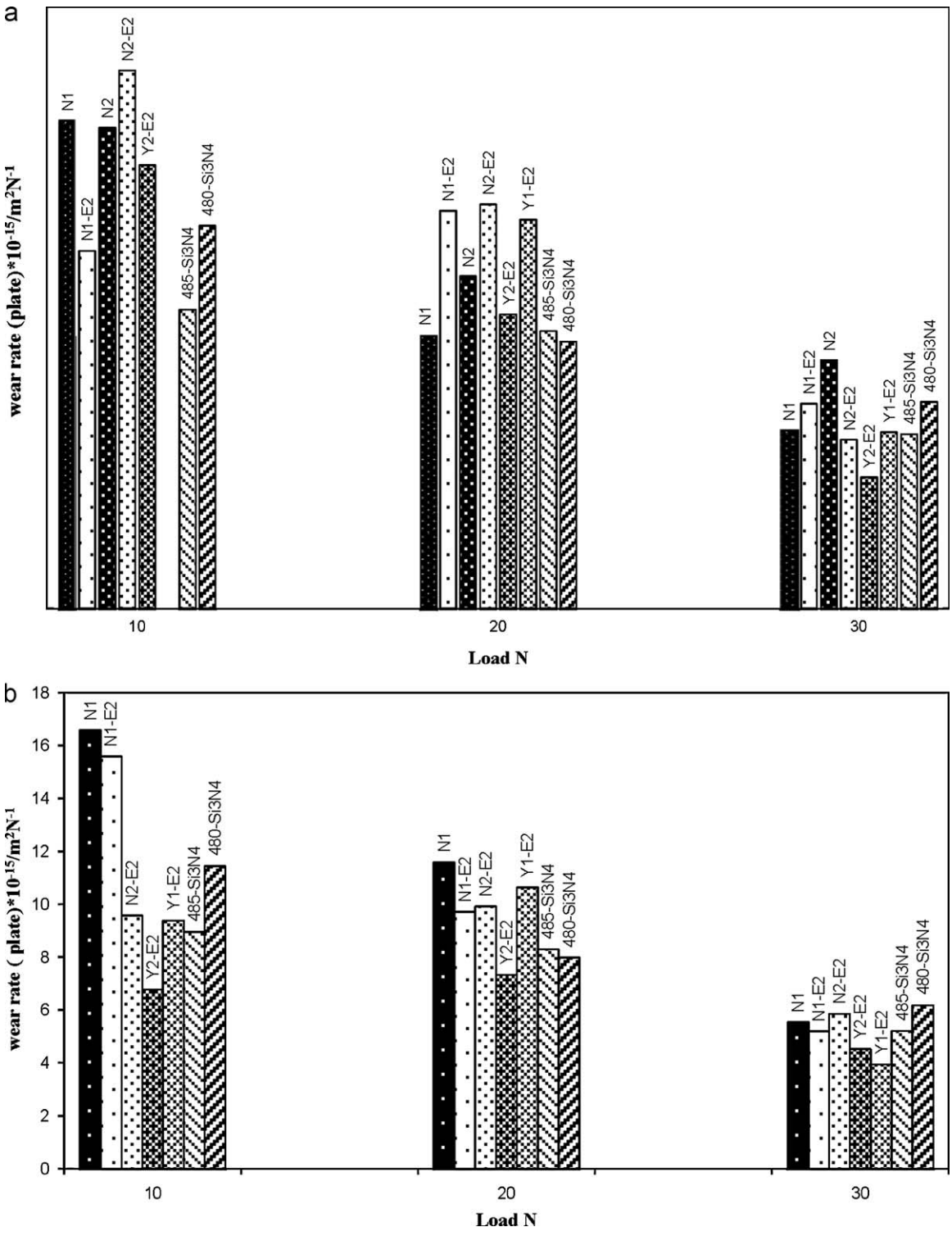

Fig. 2. Variation of the wear rate of the ceramic plate with load in (a) spark plasma sintered materials and (b) gas pressure sintered materials.

The best material, Y2-E2, showed better wear properties than the investigated β-Si_3N_4 materials, accepted as standard materials. Since the wear properties of the 485-Si_3N_4 material are better than those of the 480-Si_3N_4 material, the former was compared with the SiAlON materials. The micrographs of the worn surface of the 485-Si_3N_4 material are given in Fig. 6. Based on the microstructural observations, the wear process of the Si_3N_4 materials can be easily summarized. At first, the grain boundary phase breaks out (Fig. 6a and b) and, after stronger damage of the grain boundaries, the grains were pulled out at the surface (Fig. 6c). The β-Si_3N_4 materials 485 and 480 possess a high amount of grain boundary phase in comparison to the SiAlON

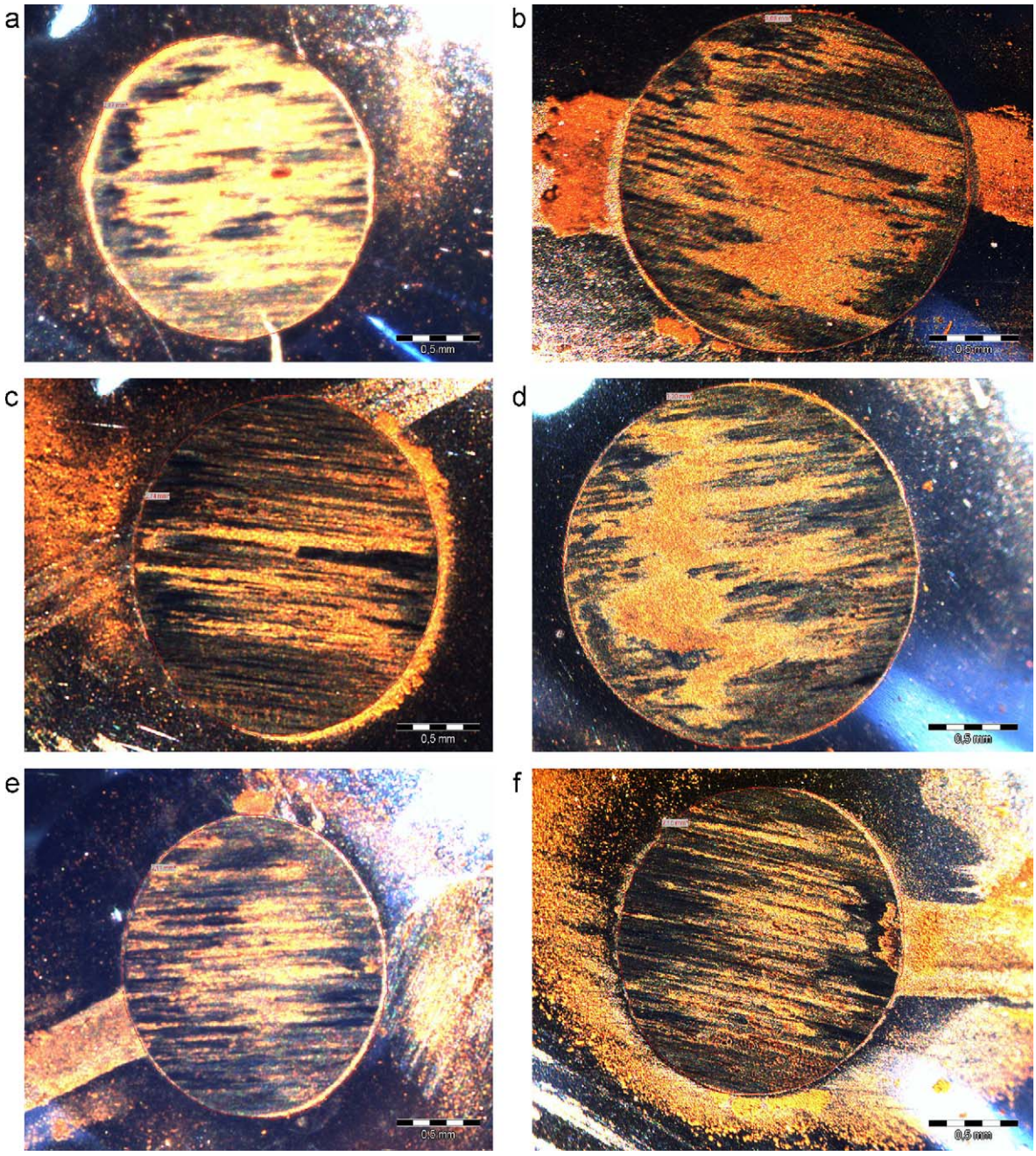

Fig. 3. The photos of wear surface of steel ball (under 30 N load) sintered by GPS (a) N1, (c) N1-E2, (e) Y1-E2, (f) Y2-E2 and sintered by SPS (b) N1 and (d) N1-E2.

materials. Thus, wear started from the grain boundary phase in the 485-Si_3N_4 material at a low load (10 N), whereas this effect could not be seen in the Y2-E2 and N1 materials, sintered using GPS or SPS, even under a high load application (30 N). Not even the higher fracture toughness of the β-Si_3N_4 materials (485 and 480), in comparison to the best SiAlON material (Y2-E2), could decelerate the wear process.

Mechanical test results showed that generally samples, sintered by SPS, have higher hardness than that of GPS samples. However, the toughness of these samples is lower than that of GPS-sintered. These results are in agreement with the friction coefficient of samples. By increasing the amount of α-SiAlON phase the friction resistance and toughness of samples decreased.

4. Discussion

The two different types of sintering methods did not showed much effect on densification behaviour of both compositions. The samples, sintered by SPS (at 1750 °C and 5 min) have higher amount of the α-SiAlON phase than that of those gas pressure sintered. This result can be explained by the instability of the α-SiAlON phase at lower temperatures (1450–1600 °C). After sintering at a high temperature, during the cooling pro-

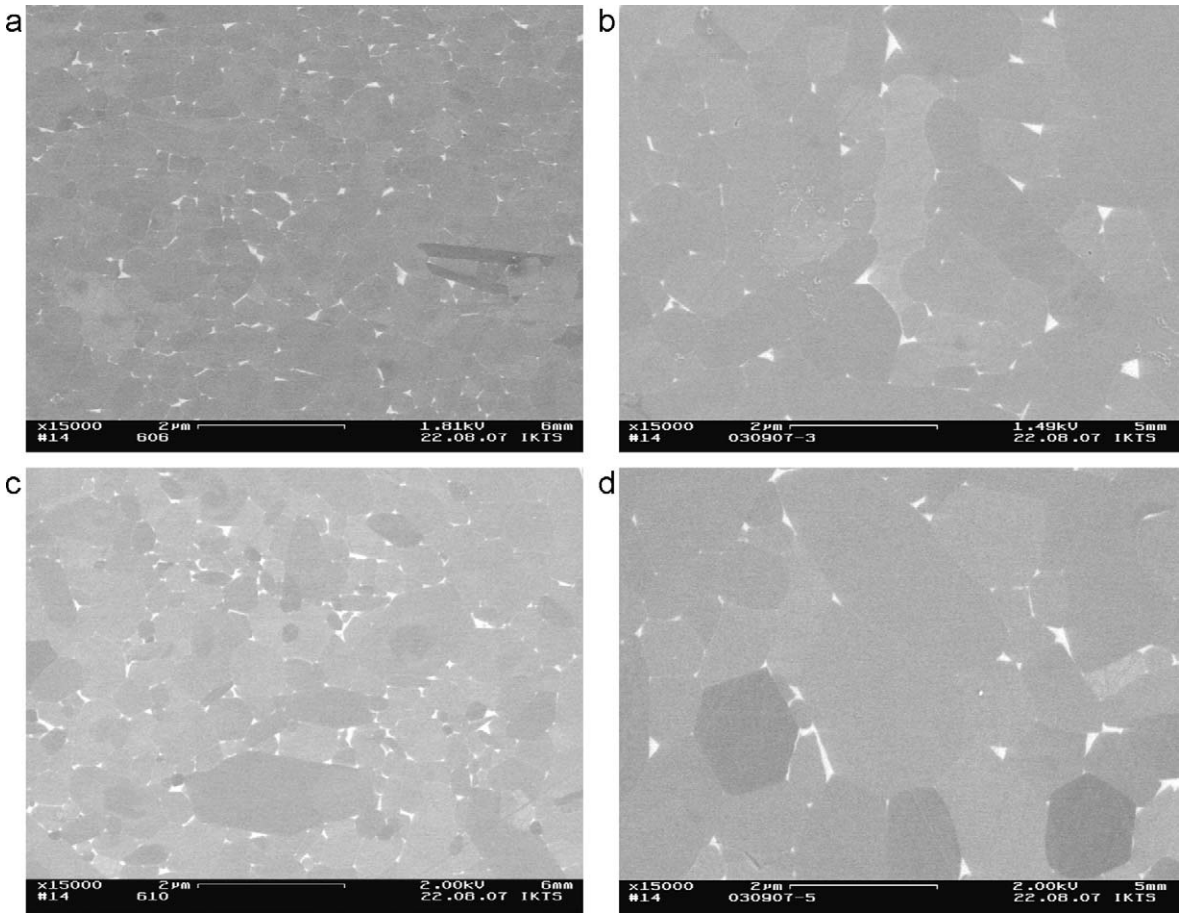

Fig. 4. FESEM micrographs of the as-sintered materials (a) SPS-N1, (b) GPS-N1, (c) SPS-Y2-E2 and (d) GPS-Y2-E2.

cess, the α → β SiAlON phase transformation occurs.[30] In the present study, there could be two effective factors influencing this transformation. The SPS system has much higher cooling rates in comparison to the GPS furnace in stabilizing the α-SiAlON phase. On the other hand, the SPS samples may not have reached equilibrium. Another factor is the presence of an amorphous phase. The stability of the α-SiAlON is related to the ionic size of the additive, and the stabilization capacity of the large cations (Nd^{3+}) in the α-SiAlON structure is lower than that of the smaller cations.[30–37] The use of an additional rare earth additive, in comparison to the α-SiAlON composition, results in a higher amount of the α-SiAlON phase in the materials (compare N2 and N2-E2) in the gas pressure sintering process.

The microstructural effect on wear behaviour on SiAlON was clearly observed in sample N1 related with sintering method. Due to coarse grain morphology and less amount of grain boundary phase sample N1, sintered by GPS, has lower wear resistance than that of SPS-sintered. It is also in agrees with the literature. Zutshi et al., Gomes et al. and Dogan and Hawk found that the wear resistance was improved when the grain size became smaller despite of a decrease in fracture toughness.[38–40] By contrast, Carrasquero et al. demonstrated that the "self-reinforced" microstructure with elongated grains suppressed the propagation of cracks, which not only improved both fracture toughness and strength but also enhanced the wear resistance.[41] In α/β-SiAlON materials a higher aspect ratio of the α- and β-SiAlON grains was observed than in single phase α-SiAlON materials. The best wear properties were achieved in the Y_2O_3 doped α/β-SiAlON composite material (Y2-E2), with a high aspect ratio and fracture toughness sintered by gas pressure sintering. Even though fine grain morphology was obtained in the spark plasma sintered materials, the aspect ratio of the grains was not high enough to improve the wear behaviour of these materials. The SiAlON materials, densified using SPS, with fine microstructure and low aspect ratios, possess lower fracture toughness in comparison to gas pressure sintered materials. Comparing the wear behaviour of the α-SiAlON materials with that of β-Si_3N_4 materials, an inferior wear behaviour for the α/β-SiAlON Y2-E2 material could be detected under a high load. This can be explained by the effect on wear behaviour of the greater grain boundary phase in β-Si_3N_4 materials. In β-Si_3N_4 materials, the grain boundary phase accelerates the wear observed in two steps:

i) by removing the grain boundary phase, and
ii) by continuing with a pull out of large grains.

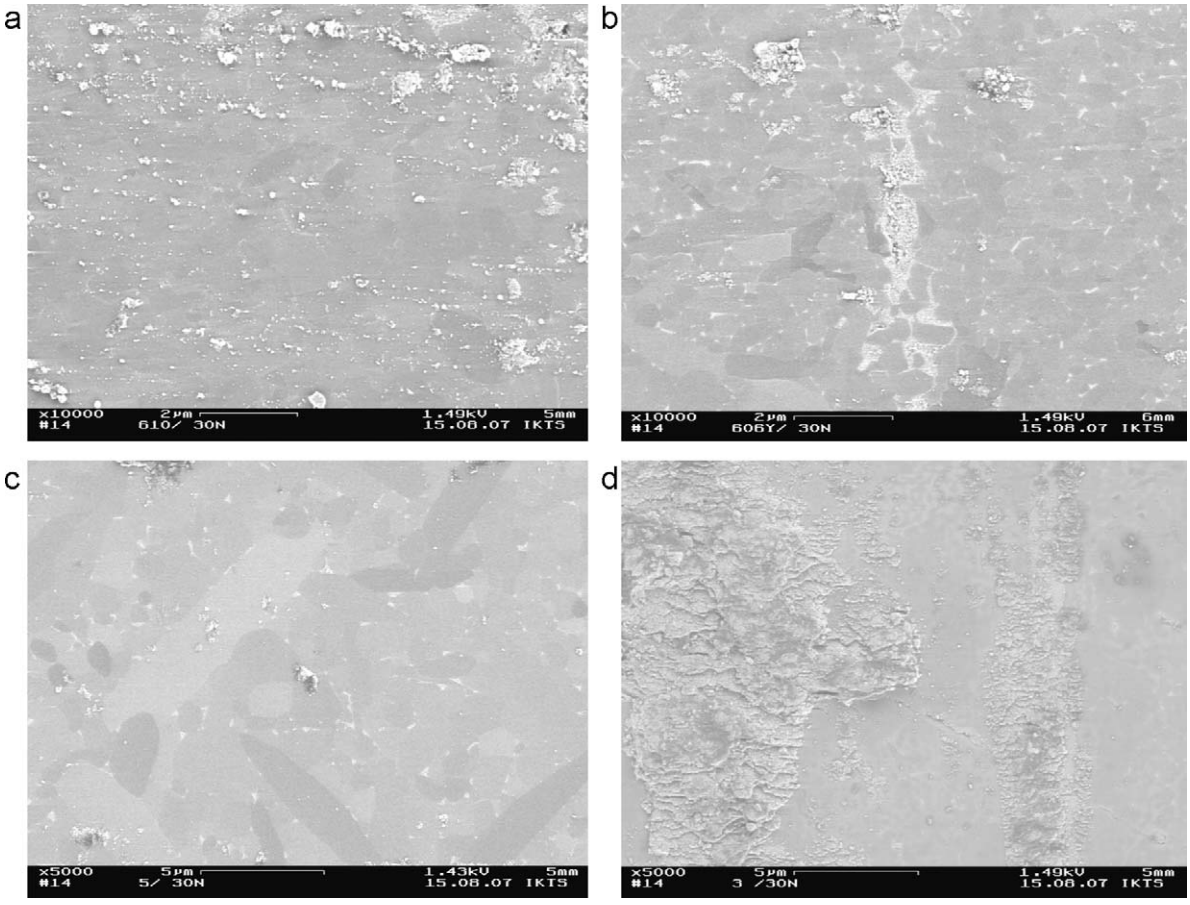

Fig. 5. FESEM micrographs of the worn material surfaces under a 30 N load (a) SPS-Y2-E2, (b) SPS-N1, (c) GPS-Y2-E2 and (d) GPS-N1.

However, this behaviour was less pronounced in the α/β-SiAlON composition (Y2-E2), sintered using GPS.

The effect of amount of sintering additive on wear behaviour of SiAlON is also clearly observed in this study. The sample N1-E2, doped with excess amount of Nd_2O_3 and sintered by SPS, has lower friction resistance than sample N1 which was sintered at same conditions. It would seem that the increase in the wear rate of the materials can not have been caused solely by the change in the amount of the grain boundary phase, but are also related to grain morphology and fracture toughness of the materials (Table 3).

In the literature, it has been shown that friction coefficient is strongly influenced by hardness and decreases as the α-SiAlON content increases.[42] In the present study, the same results were observed for N1 and Y2-E2 materials sintered by both types of sintering process. Additionally, yttrium doped materials (Y1-E2 and Y2-E2) showed a better wear rate than neodymium doped materials (N1-E2 and N2-E2). This result is related to the ionic strength of yttrium.[43]

Table 3
Hardness and toughness of materials.

Sample	SPS		GPS		Standard	
	HV10 (GPa)	K_{IC} (MPa m$^{1/2}$)	HV10 (GPa)	K_{IC} (MPa m$^{1/2}$)	HV10 (GPa)	K_{IC} (MPa m$^{1/2}$)
N1	19.01 ± 0.48	3.2	18.92 ± 0.15	4.2		
N1-E2	18.51 ± 0.19	3.3	18.74 ± 0.40	4.2		
N2	19.15 ± 0.37	3.3	–	–		
N2-E2	19.04 ± 0.14	3.7	17.90 ± 0.21	4.6		
Y1-E2	18.64 ± 0.25	3.6	18.19 ± 0.34	3.0		
Y2-E2	19.04 ± 0.24	3.6	18.21 ± 0.45	4.8		
485-Si_3N_4[a]					15.07 ± 0.23	5.8
485-Si_3N_4[b]					15.77 ± 0.17	5.5

[a] Sintered by hot pressed at 1850 °C.
[b] Sintered by hot pressed at 1700 °C.

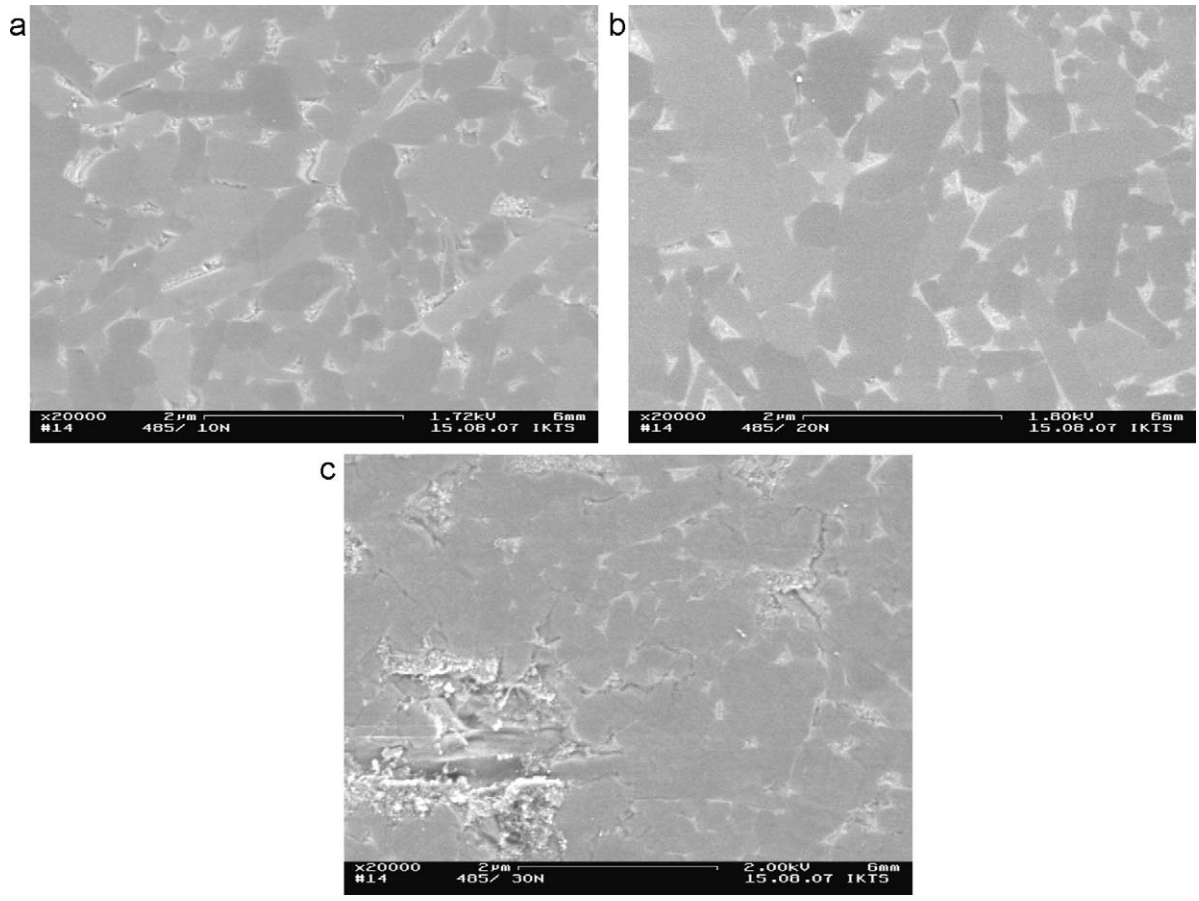

Fig. 6. FESEM micrographs of the worn area of 485-Si_3N_4 material surfaces under (a) 10 N, (b) 20 N and (c) 30 N loads.

5. Conclusion

Single phase α-SiAlON and two phase α/β-SiAlON materials have been produced using Y and Nd as stabilizing cation in SiAlON phase, and their wear properties assessed under dry sliding conditions. The type of sintering process (SPS and GPS) was shown to have a significant effect on wear behaviour.

Under high loads the better mechanical properties of compositions afforded by the presence of elongated α and β-SiAlON grains resulted in lower wear than the single α-SiAlON and α/β composite materials. This is not only related with the presence of β-SiAlON in structure but also microstructure of α-SiAlON grains, which are in elongated form.

Additionally, the additive system used in the sintering of materials affected the wear rates as Nd-doped materials under dry sliding conditions. Y2-E2 materials that have well wear resistance under different loading conditions, due to stronger interfaces, exhibited lower wear rates under high load conditions, where fracture is dominant, as a consequence of strong bonding strength between the grains and grain boundary resulting in a higher degree of brittle fracture.

Acknowledgements

This work is supported through a research grant from Deutscher Academischer Austausch Dienst (DAAD, Germany). One of the authors (S. Kurama) acknowledges financial support from DAAD. She would also like to thank the Fraunhofer Institute for Ceramic Technologies and Systems for assistance in the characterisation of materials.

References

1. Hampshire S, Park HK, Thompson DP, Jack KH. α-SiAlON ceramics. *Nature* 1978;**274**:880–2.
2. Ekstrom T, Nygren M. SiAlON ceramics. *J Am Ceram Soc* 1992;**75**:259–76.
3. Mandal H. New developments in α-SiAlON ceramics. *J Eur Ceram Soc* 1999;**19**:2349–57.
4. Izhevskyi VA, Genova LA, Bressiani AHA, Bressiani JC. Microstructure and properties tailoring of liquid-phase sintered SiC. *Int Refract Met Hard Mater* 2001;**19**:409–17.
5. Strecker K, Gonzaga R, Ribeiro S, Hoffmann MJ. Substitution of Y_2O_3 by a rare earth oxide mixture as sintering additive of Si_3N_4 ceramics. *Mater Lett* 2000;**45**:39–42.
6. Santos C, Strecker K, Baldacim SA, Silva OMM, Silva CRM. Properties of hot-pressed, partially stabilized CRE-α-SiAlONs as a function of the additive content. *Int Refract Met Hard Mater* 2004;**22**(2–3):79–85.
7. Santos C, Strecker K, Riberio S, Silva CRM. Substitution of pure Y_2O_3 by a mixed concentrate of rare earth oxides (CTR_2O_3) as sintering additive of Si_3N_4: a comparative study of the mechanical properties. *J Mater Process Technol* 2003;**142**(3):697–701.
8. Tanaka I, Kleebe HJ, Cinibulk MK, Bruley J, Clarke DR, Rühle M. Calcium concentration dependence of the intergranular film thickness in silicon nitride. *J Am Ceram Soc* 1994;**77**:911–4.

9. Huang ZK, Tien TY. Solid–liquid reaction in the system Si_3N_4–$Y_3Al_5O_{12}$–$Y_2Si_2O_7$ under 1 MPa of nitrogen. *J Am Ceram Soc* 1994;**77**:2763–6.
10. Shen Z, Nygren M. On the extension of the α-sialon phase area in yttrium and rare-earth doped systems. *J Eur Ceram Soc* 1997;**17**:1639–45.
11. Kondo N, Asayama M, Suzuki Y, Ohji T. High-temperature strength of sinter-forged silicon nitride with lutetia additive. *J Am Ceram Soc* 2003;**86**:1430–2.
12. Cinibulk MK, Thomas G, Johnson SM. Strength and creep behaviour of rare-earth disilicate–silicon nitride ceramics. *J Am Ceram Soc* 1992;**75**:2050–5.
13. Cheong DS, Sanders WA. High-temperature deformation and microstructural analysis for silicon nitride–scandium (III) oxide. *J Am Ceram Soc* 1992;**75**:3331–6.
14. Yang L, Li J, Chen Y, Dai J. Secondary crystalline phases and mechanical properties of heat-treated Si_3N_4. *Mater Sci Eng A* 2003;**363**:93–8.
15. Jones MI, Hyuga H, Hirao K, Yamauchi Y. Wear behaviour of single phase and composite sialon ceramics stabilized with Y_2O_3 and Lu_2O_3. *J Eur Ceram Soc* 2004;**24**:3271–7.
16. Jones MI, Hirao K, Hyuga H, Yamauchi Y, Kanzaki S. Wear properties of Y-α/β composite sialon ceramics. *J Eur Ceram Soc* 2003;**23**:1743–50.
17. Abo-Naf SM, Dulias U, Schneider J, Zum Gahr K-H, Holzer S, Hoffmann MJ. Mechanical and tribological properties of Nd- and Yb-SiAlON composites sintered by hot isostatic pressing. *J Mater Proc Technol* 2007;**183**:264–72.
18. Chen I-W, Rosenflanz A. A tough SiAlON ceramic based on α-Si_3N_4 with a whisker-like microstructure. *Nature* 1997;**389**:701–4.
19. Kim J, Rosenflanz A. Microstructure control of in-situ toughened α-SiAlON ceramics. *J Am Ceram Soc* 2000;**12**(7):1819–21.
20. Shen Z, Nordberg L-O, Nygren M, Ekstrom T. α-SiAlON grains with high aspect ratio-utopia or reality? In: Babini GN, Haviar M, Sajgalik P, editors. *Engineering ceramics'96: higher reliability through processing*. Dordrecht, The Netherlands: Kluwer Academic Publishers; 1997. p. 169–76.
21. Shen Z, Zhao Z, Peng H, Nygren M. Formation of tough interlocking microstructures in silicon nitride ceramics by dynamic ripening. *Nature* 2002;**417**:266–9.
22. Shen ZJ, Johnsson M, Zhao Z, Nygren M. Spark plasma sintering of alumina. *J Am Ceram Soc* 2002;**85**(8):1921–7.
23. Mishra RS, Mukherjee AK. Electric pulse assisted rapid consolidation of ultrafine grained alumina matrix composites. *Mater Sci Eng A* 2000;**287**:178–82.
24. Nishimura T, Mitomo M, Hirotsuru H, Kawahara M. Fabrication of silicon nitride nanoceramics by spark plasma sintering. *J Mater Sci Lett* 1995;**14**:1046–7.
25. Shen Z, Nygren MJ. Kinetic aspects of super fast consolidation of silicon nitride based ceramics by spark plasma sintering. *Mater Chem* 2001;**11**(1):204–7.
26. Zhan GD, Mitomo M, Xie RJ, Tanaka H. Thermal and electrical properties in plasma-activation-sintered silicon carbide with rare-earth-oxide additives. *J Am Ceram Soc* 2001;**84**(10):2448–50.
27. Salamon D, Shen Z, Sajgalik P. Rapid formation of α-SiAlON during spark plasma sintering: its origin and implications. *J Eur Ceram Soc* 2007;**27**:2541–7.
28. Taut T, Bergmann J. Rietveld-analyse mit dem programmsystem Refine++. Handbuch der version 1.1, 1999.
29. Anstis GR, Chantikul P, Lawn BR, Marshall DB. A critical evaluation of indentation techniques for measuring fracture toughness. I. Direct crack measurements. *J Am Ceram Soc* 1981;**64**(2):533–8.
30. Mandal H, Camuscu N, Thompson DP. Comparison of the effectiveness of rare earth sintering additives on the high temperature stability of α-SiAlON Ceramics. *J Mater Sci* 1995;**30**:5901–9.
31. Yu ZB, Thompson DP, Bhatti AR. α ⇔ β-SiAlON transformation in Li-sialon ceramics. *Br Ceram Trans* 1998;**97**:41–7.
32. Redington M, Hampshire S. Multi-cation alpha-SiAlONs. *Br Ceram Proc* 1992;**49**:175–90.
33. Huang ZK, Jiang YZ, Tien TY. Formation of α-SiAlONs with dual modifying cations (Li + Y and Ca + Y). *J Mater Sci Lett* 1997;**16**:747–51.
34. Dolekcekic E, Kurama S, Mandal H, Oberacher R, Hoffmann MJ, Thompson DP. Multi cation doped alpha-SiAlON. In: Turan S, Kara F, Pütün E, editors. *Proceeding of IV. Ceramic congress*. Turkey: Turkish Ceramic Society; 1998. p. 395–401.
35. Seeber AJ, Cheng Y-B. Thermal stability of mixed-cation α-SiAlON ceramics. *Mater Sci Eng A* 2003;**339**:115–23.
36. Seeber AJ, Cheng Y-B. α′ Phase stability in Nd–Li–SiAlON systems. *J Eur Ceram Soc* 2003;**23**:1083–92.
37. Kurama S, Herrmann M, Mandal H. The effect of processing conditions, amount of additives and composition on the microstructures and mechanical properties of α-SiAlON ceramics. *J Eur Ceram Soc* 2002;**22**: 109–19.
38. Zutshi A, Haber RA, Niesz DE, Adams JW, Wachtman JB, Ferber MK, et al. Processing, microstructure, and wear behavior of silicon nitride hot-pressed with alumina and yttria. *J Am Ceram Soc* 1994;**77**:883–90.
39. Gomes JR, Oliveira FJ, Silva RF, Osendi MI, Miranzo P. Effect of α-/β Si_3N_4-phase ratio and microstructure on the tribological behavior up to 700 °C. *Wear* 2000;**239**:59–68.
40. Dogan CP, Hawk JA. Microstructure and abrasive wear in silicon nitride ceramics. *Wear* 2001;**250**:256–63.
41. Carrasquero E, Bellosi A, Staia MH. Characterization and wear behavior of modified silicon nitride. *Int J Refract Met Hard Mater* 2005;**23**: 391–7.
42. Prakash B, Bandyopadhyaya S, Mukerji J. Friction coefficient of (α + β)-SiAlON composite against a steel and dense silicon nitride tribopair. *J Am Ceram Soc* 1999;**82**:2255–6.
43. Yu J, Du H, Shuba R, Chen IW. Dopant-dependent oxidation behavior of alpha-SiAlON ceramics. *J Mater Sci* 2004;**39**:4855–60.